

**Identification of miR-145 as a key regulator involved in LC-PUFA biosynthesis  
by targeting *hnf4a* in the marine teleost *Siganus canaliculatus***

Cuiying Chen<sup>#1\*</sup>, Mei Zhang<sup>#1</sup>, Yuanyou Li<sup>2</sup>, Shuqi Wang<sup>1,3</sup>, Dizhi Xie<sup>2</sup>, Xiaobo Wen<sup>1,2</sup>,  
Yu Hu<sup>1</sup>, Jiajian Shen<sup>1</sup>, Xianda He<sup>1</sup>, Cuihong You<sup>1</sup>, Douglas R. Tocher<sup>4</sup>, and Óscar  
Monroig<sup>5</sup>

<sup>1</sup> Guangdong Provincial Key Laboratory of Marine Biotechnology, Institute of Marine  
Sciences, Shantou University, Shantou 515063, China;

<sup>2</sup> School of Marine Sciences of South China Agricultural University & Guangdong  
Laboratory for Lingnan Modern Agriculture, Guangzhou 510642, China;

<sup>3</sup> Research Center for Nutrition & Feed and Healthy Breeding of Aquatic Animals of  
Guangdong Province, Shantou 515063, China;

<sup>4</sup> Institute of Aquaculture, Faculty of Natural Sciences, University of Stirling, Stirling  
FK9 4LA, Scotland, UK;

<sup>5</sup> Instituto de Acuicultura Torre de la Sal, Consejo Superior de Investigaciones  
Científicas (IATS-CSIC), 12595 Ribera de Cabanes, Castellón, Spain.

<sup>#</sup> Contributed equally to this work.

**\*Corresponding Author**

Cuiying Chen, Ph.D. (E-mail: [cychen@stu.edu.cn](mailto:cychen@stu.edu.cn))

Institute of Marine Sciences, Shantou University, 243 DaXue Road, Shantou 515063,  
China.

## Abstract

Fish, particularly marine species, are considered as the major source of long-chain polyunsaturated fatty acids (LC-PUFA) in the human diet. The extent to which fish can synthesize LC-PUFA varies with species and is regulated by dietary fatty acids and ambient salinity. Therefore, in order to enable fish to produce more LC-PUFA, comprehending the mechanisms underlying the regulation of LC-PUFA biosynthesis is necessary. Here, the regulatory roles of miR-145 were investigated in the marine teleost rabbitfish *Siganus canaliculatus*. The hepatic abundance of miR-145 was lower in rabbitfish reared in low salinity (10 ppt) in comparison with that of those cultured in seawater (32 ppt), while the opposite pattern was observed for transcripts of the transcription factor hepatocyte nuclear factor 4 alpha (Hnf4 $\alpha$ ), known to affect rabbitfish LC-PUFA biosynthesis. Rabbitfish *hnf4 $\alpha$*  was identified as a target of miR-145 by luciferase reporter assays, and overexpression of miR-145 in *S. canaliculatus* hepatocyte line (SCHL) markedly reduced expression of Hnf4 $\alpha$  and its target genes involved in LC-PUFA biosynthesis, namely  $\Delta 4$  *fads2*,  $\Delta 6\Delta 5$  *fads2* and *elovl5*. The opposite pattern was observed when miR-145 was knocked down in SCHL cells, with these effects being attenuated by subsequent *hnf4 $\alpha$*  knockdown. Moreover, increasing endogenous Hnf4 $\alpha$  by knockdown of miR-145 increased expression of LC-PUFA biosynthesis genes and enhanced synthesis of LC-PUFA in both SCHL cells and rabbitfish *in vivo*. This is the first report to identify miR-145 as a key effector of LC-PUFA biosynthesis by targeting *hnf4 $\alpha$* , providing a novel insight into mechanisms of regulation of LC-PUFA biosynthesis in vertebrates.

45    **Keywords:** miR-145, *hnf4α*, LC-PUFA biosynthesis, *Siganus canaliculatus*

## 1. Introduction

Arachidonic acid (ARA; 20:4n-6), eicosapentaenoic acid (EPA; 20:5n-3) and docosahexaenoic acid (DHA; 22:6n-3), which belong to long-chain polyunsaturated fatty acids (LC-PUFA,  $\geq C_{20}$  and  $\geq 2$  double bonds), are vital for human health having beneficial impacts in several pathologies including cardiovascular and inflammatory diseases, with DHA in particular having further key roles in neural development.<sup>1-3</sup> Since human beings have limited capability to endogenously biosynthesize LC-PUFA to meet physiological demands, dietary intake of these health-promoting fatty acids is necessary.<sup>4</sup> Marine fish, particularly oily species, are major sources of n-3 LC-PUFA in humans,<sup>5</sup> and this has prompted considerable attention to understand LC-PUFA biosynthesis pathways in fish.<sup>6</sup>

The extent that fish can endogenously synthesize LC-PUFA varies with species and is affected by many other factors including age, gender, and gene polymorphisms.<sup>5-</sup>

<sup>7</sup> Generally, freshwater fish and salmonids have the capability to biosynthesize LC-PUFA from  $C_{18}$  precursors, namely linoleic acid (LA; 18:2n-6) and alpha-linolenic acid (ALA; 18:3n-3), via sequential desaturation and elongation reactions catalyzed by fatty acid desaturases (Fads) and elongation of very long-chain fatty acids (Elovl) proteins, respectively. With few exceptions,<sup>8</sup> Fads2 represents the sole Fads-like desaturase found in teleosts, although enzymatic activities of teleost Fads2 include  $\Delta 8$ ,  $\Delta 6$ ,  $\Delta 5$  and  $\Delta 4$  desaturase specificities. With regard to elongases, Elovl2, Elovl4, Elovl5 and Elovl8b have been shown to be involved in PUFA elongation.<sup>5,7,9</sup> Many marine teleosts are inefficient in LC-PUFA biosynthesis or even lack the ability, due to the absence of

key LC-PUFA biosynthetic enzymes.<sup>5-7</sup> At present, the decline in wild fisheries means aquaculture now supplies an increasing amount of the key n-3 LC-PUFA in human diets.<sup>10</sup> However, with the growth of aquaculture, using large amounts of fish oil (FO), the traditional source of lipid used to supply n-3 LC-PUFA in aquaculture feeds, is now recognized as an increasingly environmentally unsustainable and economically unfeasible.<sup>6,11</sup> Although vegetable oils (VO) are more sustainable and, therefore, ideal alternatives to substitute for dietary FO, they are short of LC-PUFA but often rich in C<sub>18</sub> PUFA.<sup>12,13</sup> Therefore, with the inclusion levels of VO increasing in feeds for farmed marine species, it is very important to elucidate pathways in fish for the endogenous biosynthesis of LC-PUFA biosynthesis so that conversion of the C<sub>18</sub> PUFA, enriched in VO, to LC-PUFA can be enhanced to both satisfy the physiological requirements of the fish themselves and guarantee product quality for humans.

The herbivorous rabbitfish, *S. canaliculatus*, was the first marine teleost shown to have  $\Delta 6\Delta 5$  Fads2,  $\Delta 4$  Fads2, Elovl5, Elovl4 and Elovl8b enzymes enabling rabbitfish to produce LC-PUFA from C<sub>18</sub> PUFA precursors.<sup>9,14,15</sup> Thus, rabbitfish is a potential model species to study mechanisms of regulation of LC-PUFA biosynthesis in marine fish. There has been considerable research effort to fully understand the mechanisms of LC-PUFA biosynthesis regulation in rabbitfish that arguably, along with Atlantic salmon *Salmo salar*, represents the teleost species in which the mechanisms are best understood. It has been established that the expression and enzyme activities of LC-PUFA synthesis related genes are controlled by both nutritional and environmental factors including dietary lipids/fatty acids and salinity, respectively,<sup>16,17</sup> and *fads* and

*elovl* genes generally show increased expression in fish grown in low salinity or fed diets based on VO (lacking LC-PUFA but with abundant C<sub>18</sub> PUFA).<sup>15-18</sup> Furthermore, a range of transcription factors, including sterol regulatory element binding protein 1 (Srebp1),<sup>19</sup> stimulatory protein 1 (Sp1),<sup>20</sup> and peroxisome proliferator-activated receptor gamma (Pparγ)<sup>21</sup> were been implicated in regulating LC-PUFA biosynthesis by directly controlling *fads* and *elovl* gene transcription.

Hepatic nuclear factor 4 alpha (Hnf4α), a member of the nuclear receptor superfamily enriched in liver, binds as a homodimer to its DNA recognition site, a direct repeat element (AGGTCA) with a spacing of one or two nucleotides (DR1 or DR2).<sup>22</sup> It plays major roles in liver development, differentiation and metabolism through controlling the expression of many genes expressed in the liver, and some genes that Hnf4α regulates are associated with a number of critical metabolic pathways, such as fatty acid synthesis and oxidation, lipid transport, steroid metabolism, lipoprotein metabolism and glucose metabolism.<sup>23-25</sup> Moreover, we recently found that Hnf4α was also involved in regulating the biosynthesis of LC-PUFA in *S. canaliculatus* through transcriptionally regulating desaturase and elongase enzyme genes, including Δ4 *fads2*, Δ6Δ5 *fads2* and *elovl5*.<sup>26-28</sup>

Furthermore, our recent work has shown that the expression of *fads* and *elovl* is also regulated directly or indirectly by microRNAs (miRNA or miR) at the post-transcriptional level in rabbitfish *S. canaliculatus*,<sup>29-34</sup> highlighting the vital regulatory roles of miRNAs in regulating biosynthesis of LC-PUFA in vertebrates. MiRNAs, small non-coding RNA molecules, regulate expression of genes through binding 3'

untranslated regions (3'UTR) of mRNAs post-transcriptionally, and they are now appreciated as key regulators of cell proliferation, differentiation, metabolism and inflammation.<sup>35,36</sup> Recently, miRNAs were shown to have impacts on lipid and lipoprotein metabolism,<sup>37-39</sup> and we have reported that certain miRNAs, namely miR-17, miR-24, miR-26a, miR-33 and miR-146a play pivotal roles in the regulation of LC-PUFA biosynthesis in the rabbitfish.<sup>29-34</sup> A further microRNA, miR-145, has been shown to be involved in cholesterol metabolism and adipogenesis in mammals.<sup>40-42</sup> For example, miR-145 increased cholesterol level in islets through decreasing ATP-binding cassette transporter A1 (ABCA1) expression in murine islets,<sup>40</sup> and attenuated lipolysis by directly targeting Foxo1 (forkhead box O1) and Cgi58 (comparative gene identification 58, also known as alpha/beta hydrolase domain 5, ABHD5) in white adipose tissue of mice.<sup>42</sup> However, the roles of miR-145 in LC-PUFA biosynthesis regulation in vertebrates still requires clarification. Therefore, the overall aim of the present study was to characterize and clarify the roles of miR-145 in LC-PUFA biosynthesis and its regulation by targeting *hnf4α* in rabbitfish. In the present study, we found a conserved complementary site for miR-145 in the 3'UTR of *hnf4α* mRNA in rabbitfish, which led us to speculate that *hnf4α* might be a novel target of miR-145 and that, consequently, Hnf4α and miR-145 may interact to regulate LC-PUFA biosynthesis.

## **2. Materials and methods**

### **2.1 Ethics statement**

Rabbitfish juveniles (~10-20 g) used for both the feeding trial and *in vivo* miRNA

antagomir injection experiment were obtained from wild environments near the coast near Nan Ao Marine Biology Station (NAMBS) of Shantou University, Southern China. All procedures performed on fish complied with the National Institutes of Health guide for the care and use of laboratory animals (NIH Publications No. 8023, revised 1978) and were approved by the Institutional Animal Care and Use Committee of Shantou University (Guangdong, China).

The feeding experiment was conducted at NAMBS. The ingredients and proximate compositions of the experimental diets were provided previously.<sup>17</sup> Liver tissues from rabbitfish juveniles fed two diets containing two lipid sources (FO and VO) and reared at two salinities (10 and 32 ppt) were used in the present study (for details see Chen et al.<sup>31</sup>). At the end of the 8-week feeding trial, fish were fasted for 24 h and subsequently anesthetized with 0.01 % 2-phenoxyethanol (Sigma-Aldrich, USA) prior to liver tissues excision (six fish per tank), frozen in liquid nitrogen, and subsequently stored at -80 °C prior to further analysis.

## **2.2 Reagents, cells and antibodies**

The *S. canaliculatus* hepatocyte line (SCHL), initially established in 2017,<sup>43</sup> was maintained at 28 °C in a normal atmosphere incubator in Dulbecco's modified Eagle's medium/nutrient F12 (DMEM/F12, Gibco, USA) supplementing with 20 mM 4-(2-hydroxyethyl) piperazine-1-ethanesulphonic acid (HEPES, Sigma-Aldrich, USA), 10 % fetal bovine serum (FBS, Gibco), 0.2 % rainbow trout *Oncorhynchus mykiss* serum (Caisson Labs), 100 U ml<sup>-1</sup> streptomycin (Sigma-Aldrich) and 100 U ml<sup>-1</sup> penicillin (Sigma-Aldrich, USA). Human embryonic kidney cells (HEK 293T) (Chinese Type



Culture Collection, China) were cultured in DMEM (Gibco) containing 10 % FBS and maintained at 37 °C with 5 % CO<sub>2</sub>. The mouse monoclonal antibody against *S. canaliculatus* Δ4 Fads2 and rabbit polyclonal antibody against *S. canaliculatus* Hnf4α were customized by Abmart (Shanghai, China) and Wanleibio (Shenyang, China), respectively, while the mouse monoclonal antibody against β-actin (~42 kDa; WL01372) was obtained from Wanleibio (Shenyang).

### **2.3 Real-time quantitative PCR (qPCR)**

To examine the expression of miRNA and genes involved in LC-PUFA biosynthesis, total RNA was extracted with TRIzol reagent (Invitrogen, USA) following the manufacturer's protocol. The first-strand cDNA of miRNAs and mRNAs were generated using miRNA 1st strand cDNA Synthesis Kit (Vazyme, China) and HiScript<sup>®</sup> II Q RT SuperMix for qPCR (Vazyme), respectively. The expression of miR-145 was determined using miRNA Universal SYBR<sup>®</sup> qPCR Master Mix (Vazyme) with miR-145 specific primer and universal primer following the manufacturer's protocol. For qPCR measurement of genes (*hnf4α*, Δ4 *fads2*, Δ6Δ5 *fads2* and *elovl5*), LightCycler<sup>®</sup> 480 SYBR Green I Master (Roche, Germany) was used with gene-specific primers. All real-time qPCR reactions were carried out on the LightCycler<sup>®</sup> 480 thermocycler (Roche).<sup>26</sup> The expression levels of all LC-PUFA biosynthesis related genes were normalized with that of *β-actin*, and levels of miR-145 were normalized with 18S rRNA. Triplicate wells were used per sample and the primer sequences used for qPCR were presented at Supporting Table S1.

### **2.4 Plasmid construction**

To construct the wild-type (WT) 3'UTR-luciferase plasmid of *hnf4α*, the whole 3'UTR of the rabbitfish *hnf4α* (JF502073.1) gene was cloned, and the DNA fragment was inserted into the dual-luciferase reporter vector pmirGLO (Promega, USA) by digestion with restriction endonucleases *Sac* I and *Xba* I (New England Biolabs, Ipswich, MA, USA). The mutant-type (MU) *hnf4α*-3'UTR reporter vector was obtained using *Muta-direct*<sup>TM</sup> site-directed mutagenesis kit (SBS Genetech, China). The pre-miR-145 sequence, obtained by genome walking technology as described previously,<sup>29</sup> was digested by *EcoR* I and *BamH* I and inserted into the pEGFP-C3 vector (Clontech, USA) to obtain the pre-miRNA expression plasmid. Additionally, the 22 nt oligonucleotide with 100 % match to miR-145 was generated and ligated into pmirGLO as the positive control plasmid (pmirGLO-R145), and an empty pmirGLO vector (pmirGLO-empty) was used as the negative control. After construction, the high-purity plasmid isolation kit (Roche) was used to isolate the recombinant plasmids and the insert fragments of recombinant plasmids were sequenced by Sangon Biotech (Shanghai, China). The sequences of primers and oligonucleotides used for cloning are shown in Supporting Table S1.

## **2.5 Transfection of miRNA precursor, antagomir or siRNA**

The miR-145 precursor, miR-145 antagomir and the corresponding negative control oligonucleotides were synthesized by Hippobio (Huzhou, China). MiRNA antagomirs are chemically modified anti-sense oligonucleotides complementary to the mature miRNAs that can inhibit the function of target miRNAs and are stable *in vivo* for at least 2 weeks.<sup>44</sup> Rabbitfish SCHL cells seeded into six-well plates or 90 mm

vessels, were grown for overnight to 80-90 % confluence in DMEM/F12 supplemented with 5 % FBS and 0.1 % rainbow trout serum, and then transfected in triplicate wells with ~10-20 nM of miR-145 precursors, antagomir and corresponding negative control oligonucleotides using Lipofectamine 2000<sup>TM</sup> (Invitrogen). The small interfering RNA (siRNA) duplexes obtained from Hippobio (Huzhou) were used to silence the rabbitfish *hnf4α* expression with the following sequences: si-*hnf4α* sense, 5'-UGGAUGAGUGCGUUGAUGGTT-3'; si-*hnf4α* antisense, 5'-AACCAUCAACGCACUCAUCCA-3'. The rabbitfish SCHL cells were seeded into 90 mm vessels overnight and subsequently transfected with 50 nM of each siRNA using Lipofectamine 2000<sup>TM</sup>. Cells were harvested on 24- or 48-hour post transfection for qPCR and Western blotting analyses, respectively.

## **2.6 Dual luciferase reporter assays**

To determine whether *hnf4α* was a target gene of miR-145, a dual luciferase assay was performed using HEK 293T cells. HEK 293T cells were co-transfected with *hnf4α*-3'UTR WT or MU luciferase reporter vectors, along with pre-miR-145 plasmid, antagomir and corresponding negative controls. HEK 293T cells were seeded in 96-well plates, grown for overnight to 80 % confluence and then transfected with 100 ng of plasmids or 100 nM oligonucleotides using Lipofectamine 2000<sup>TM</sup> according to the manufacturer's instructions. Firefly and Renilla luciferase activities were quantified after 48 h transfection using a dual-luciferase reporter assay system (Promega, USA) following the manufacturer's instructions. The Firefly luciferase activities were

normalized with the Renilla luciferase activities. Six replicate wells were used for each treatment and at least two independent experiments were conducted.

## **2.7 *In vivo* miR-145 antagomir injection experiment**

The rabbitfish juveniles (~10-15 g) were kept in an indoor seawater (32 part per thousand, ppt) tank for 2 weeks to acclimatize to experimental facilities at NAMBS, and then acclimated from seawater to brackish water (10 ppt) for a further 2 weeks. Next, the rabbitfish were randomly divided into two groups (8 fish per group). The group treated with miR-145 antagomir was the experiment group, while the other treated with the negative control antagomir was set as the control group. Fish were injected into their abdominal cavity with 100 µl volume of total antagomirs diluted in PBS to 50 nmol/ml twice weekly for 3 weeks. Fish were fed a commercial diet during the *in vivo* injection experiment and the details of the fatty acid composition of the diet were described previously by Chen et al.<sup>34</sup> At 21 d post-injection, fish were fasted for 24 h and anesthetized with 0.01 % 2-phenoxyethanol (Sigma-Aldrich), and then eyes, brain, liver and muscle tissues from each fish were collected, dipped immediately into liquid nitrogen and stored at -80 °C for subsequent extraction of total RNA, proteins and lipids.

## **2.8 *Analysis of fatty acid profiles in cells and tissues***

The ALA (18:3n-3) (Cayman, USA) / BSA complex (10 mM fatty acid concentration and 10 % BSA) was prepared according to Ou et al.,<sup>45</sup> and stored at -20 °C. After being seeded into 90 mm vessels or six-well plates and overnight incubation in DMEM/F12 supplemented with 5 % FBS and 0.1 % rainbow trout serum,

SCHL cells in quadruplicate were subsequently transfected with 20 nM miR-145 antagomir or negative control antagomir (NC antagomir) using Lipofectamine 2000<sup>TM</sup>. At 24 h post transfection, cells were incubated with 30  $\mu$ M ALA/BSA complex for further 48 h and subsequently harvested for qPCR, Western blotting and fatty acid composition analyses.

Total lipid of SCHL cells and tissues was extracted with a 2:1 (v/v) mixture of chloroform / methanol containing 0.01 % butylated hydroxytoluene as antioxidant and then saponified at 65 °C for 1 h with 0.5 M potassium hydroxide in methanol. Fatty acid methyl esters (FAME) were prepared from total lipid by transesterification with boron trifluoride methanol (ca. 14 %, Acros Organics, NJ, USA), and then separated using a gas chromatography (GC-2010 plus; Shimadzu, Japan) equipped with an auto-sampler and a hydrogen flame ionization detector. The detailed GC parameters were as described previously.<sup>14</sup> Individual FAME were identified by comparing with known commercial standards (Sigma-Aldrich) and quantified using a CLASS-GS10 GC workstation (Shimadzu, Japan). The content of each FAME (mg) per dry weight of tissues (g) was calculated using a 17:0 internal standard (Sigma Aldrich).

## **2.9 Western blotting**

RIPA Buffer (ThermoFisher, USA) was used to lyse the tissues and cultured cells samples and then the lysate was centrifuged at 12000 g for 10 min at 4 °C. The protein concentration of the supernatant was determined, and then aliquots of protein (20 - 40  $\mu$ g) were loaded on a 10 % sodium dodecyl sulfate-polyacrylamide gel (SDS-PAGE) and subsequently transferred to 0.45  $\mu$ m polyvinylidene difluoride membranes (Roche,

Switzerland). After incubating at room temperature for 1 h in blocking buffer TBST, which contained 5 % non-fat milk and 0.05 % Tween-20, the membranes were incubated at 4 °C overnight with antibodies diluted in blocking buffer. Next, the membranes were washed three times with TBST buffer for 15 min and then incubated for 1 h with the appropriate secondary antibodies (HRP Goat anti-Rabbit/Mouse IgG; Abcam, USA) at room temperature. The immunoreactive bands were measured using the Odyssey infrared imaging system 2.1 (LI-COR, USA) and analyzed by Image Studio Software (version 5.2, LI-COR). The optical density of immunoreactive bands were normalized to the protein level of  $\beta$ -actin for statistical analysis.

## **2.10 Statistical analysis**

The relative expression of the genes was calculated using the  $2^{-\Delta CT}$  or  $2^{-\Delta\Delta CT}$  methods. Comparative analysis of data was carried out by the independent samples *t* test between pairs of groups or one-way analysis of variance followed by Tukey's test for multiple groups using IBM SPSS Statistics version 19.0 (SPSS Inc, Chicago, IL). All data were shown as means  $\pm$  SEM. Differences were regarded as significant when  $P < 0.05$  and highly significant when  $P < 0.01$ .

## **3. Results**

### **3.1. The abundance profile of miR-145 and hnf4 $\alpha$ mRNA**

The abundance of miR-145 was markedly lower in liver of rabbitfish reared in water at a salinity of 10 ppt compared to 32 ppt when the fish were fed with a VO-based diet (Fig. 1A). In contrast, the expression of *hnf4 $\alpha$*  in liver of fish reared at 10 ppt was

significantly higher than that in fish reared at 32 ppt (Fig. 1B). Fish fed with a VO-based diet also showed higher *hnf4a* expression than that of fish fed with the FO-based diet at both 10 and 32 ppt salinities (Fig. 1B). However, irrespective of salinity, the level of miR-145 was lower in liver of fish fed with the VO-based diet than that of fish fed with FO-based diet (Fig. 1A). The distribution of miR-145 in rabbitfish tissues showed that miR-145 expression was high ( $\Delta C_t < 5$ ) in all detected tissues with higher abundance of miR-145 in intestine and gill, while abundance was lower in spleen, heart, eyes, brain, kidney, liver and muscle (Fig. 2). However, *hnf4a* showed higher abundance in liver and eyes.<sup>28</sup>

### **3.2 Rabbitfish *hnf4a* is a target of miR-145**

A dual luciferase assay was carried out to examine the responsiveness of rabbitfish *hnf4a* 3'UTR to miR-145. The entire 3'UTR of *hnf4a* mRNA (including the miR-145 target site) was cloned into the pmirGLO luciferase reporter vector to construct a 3'UTR report plasmid (Fig. 3A). The sequence of rabbitfish pre-miR-145 was cloned and inserted into the pEGFP-C3 vector to construct the pre-miR-145 plasmid (Fig. 3B). Results from the qPCR analysis showed that HEK 293T cells transfected with the pre-miR-145 plasmid had around 8000-fold higher level of miR-145 than that of the endogenous background (Fig. 3C). As shown in Fig. 3D, there was no significant difference in the negative control group, while the positive control group of cells co-transfected with the pre-miR-145 expression plasmid and pmirGLO-R145 plasmid showed significantly lower normalized Luc activities than the pEGFP-C3 and pmirGLO-R145 co-transfected group. Additionally, the pre-miR-145 plasmid markedly

decreased luciferase activities when *hnf4α*-3'UTR-WT reporter plasmid was co-transfected into HEK 293T cells, however, this effect was largely restricted for the co-transfected plasmid containing *hnf4α*-3'UTR-MU region. Moreover, miR-145 antagomir could antagonize the inhibitory effect of pre-miR-145 on luciferase activity (Fig. 3E). These findings suggested that miR-145 directly interacted the 3'UTR of *hnf4α* mRNA and, therefore, the *hnf4α* was a target of miR-145.

### ***3.3 MiR-145 decreased the expression of hnf4α at both mRNA and protein levels***

To further determine the role of miR-145 in the regulation of *hnf4α* expression, we transfected miR-145 precursor or antagomir into SCHL cells, and then measured the mRNA and protein levels of *hnf4α*. As shown in Fig. 4A, transfection with miR-145 precursor markedly decreased expression of *hnf4α* at both mRNA and protein levels in a dose-dependent manner. In contrast, transfection with the miR-145 antagomir significantly induced *Hnf4α* expression at both mRNA and protein levels as compared with that of the negative control (Fig. 4B). These results demonstrated that miR-145 can decrease *Hnf4α* abundance at both mRNA and protein levels, indicating that miR-145 regulated the expression of endogenous *hnf4α* through both translation inhibition and mRNA degradation.

### ***3.4. MiR-145 down-regulated hnf4α resulting in decreased expression of genes involved in LC-PUFA biosynthesis***

Given that miR-145 targets and down-regulates *hnf4α*, we then investigated whether overexpression of miR-145 promoted the expression of genes encoding key enzymes of the rabbitfish LC-PUFA biosynthesis, namely  $\Delta 4$  *fads2*,  $\Delta 6\Delta 5$  *fads2* and



*elovl5*. These genes have been demonstrated to be transcriptionally regulated by Hnf4 $\alpha$  in rabbitfish.<sup>26-28</sup> Overexpression of miR-145 down-regulated the mRNA expression of *hnf4 $\alpha$*  and  $\Delta 4$  *fads2* and reduced their corresponding protein levels in SCHL cells (Fig. 5A, B). Moreover, overexpression of miR-145 in SCHL cells significantly decreased the mRNA expression levels of other Hnf4 $\alpha$  target genes including  $\Delta 6\Delta 5$  *fads2* and *elovl5* (Fig. 5B). Conversely, knockdown of miR-145 by transfecting miR-145 antagomir into SCHL cells significantly up-regulated the expression of Hnf4 $\alpha$  and its downstream target LC-PUFA biosynthesis genes,  $\Delta 4$  *fads2*,  $\Delta 6\Delta 5$  *fads2* and *elovl5* (Fig. 5A, C). These results suggested that the regulation of *hnf4 $\alpha$*  towards the genes of LC-PUFA biosynthesis was itself modulated by miR-145. To confirm this, the endogenous expression of *hnf4 $\alpha$*  was induced by transfecting SCHL cells with miR-145 antagomir and then subsequently using siRNA for knockdown. The miR-145 antagomir up-regulated levels of both Hnf4 $\alpha$  and  $\Delta 4$  Fads2 proteins, and this was attenuated by *hnf4 $\alpha$*  knockdown (Fig. 5D). The above results confirmed that miR-145 down-regulated the expression of genes encoding key enzymes involved in LC-PUFA biosynthesis by targeting *hnf4 $\alpha$* .

### ***3.5 Up-regulation of hnf4 $\alpha$ by knockdown of miR-145 increased LC-PUFA biosynthesis in ALA-treated rabbitfish SCHL cells in vitro***

Whether increasing *hnf4 $\alpha$*  by miR-145 knockdown affected biosynthesis of LC-PUFA was assessed in SCHL cells *in vitro*. Thus, SCHL cells were transfected with miR-145 antagomir or negative control (NC) antagomir for 24 h before supplementation with the precursor ALA. After incubation with ALA for further 48 h,

we observed increased *hnf4α*,  $\Delta 4$  *fads2*,  $\Delta 6\Delta 5$  *fads2* and *elovl5* mRNA levels of around 1.8- to 3.5-fold in cells receiving miR-145 antagomir compared to levels in cells receiving NC antagomir (Fig. 6A), along with increased Hnf4α and  $\Delta 4$  Fads2 protein levels (Fig. 6B). Moreover, significantly higher accumulation of LC-PUFA, such as 20:4n-6, 20:5n-3 and 22:6n-3, was observed in SCHL cells transfected with miR-145 antagomir compared to NC antagomir-treated cells (Table 1). The results indicated that knockdown of miR-145 increased the expression of *hnf4α* and subsequently promoted biosynthesis of LC-PUFA in hepatocytes of rabbitfish via up-regulating genes ( $\Delta 4$  *fads2*,  $\Delta 6\Delta 5$  *fads2* and *elovl5*) for crucial enzymes.

### **3.6 Knockdown of miR-145 promoted LC-PUFA biosynthesis in rabbitfish in vivo**

To further identify the regulatory role of miR-145 in rabbitfish LC-PUFA biosynthesis *in vivo*, miR-145 antagomir was injected into the abdomen of juvenile rabbitfish. After 3 weeks, the Western blotting of liver samples showed the protein levels of Hnf4α and  $\Delta 4$  Fads2 in the miR-145 antagomir treatment group were higher than those of the NC group (Fig. 7A). Moreover, 4~7-fold higher mRNA levels of hepatic *hnf4α*,  $\Delta 4$  *fads2*,  $\Delta 6\Delta 5$  *fads2* and *elovl5* were observed in rabbitfish after receiving the miR-145 antagomir in comparison with the NC antagomir group (Fig. 7B). Similar results were observed in brain and eyes, with the mRNA levels of *hnf4α*,  $\Delta 4$  *fads2*,  $\Delta 6\Delta 5$  *fads2* and *elovl5* higher than the levels observed in the group receiving the NC antagomir (Fig. 7C, 7D). Compared to the NC group, significantly higher contents of 20:4n-6 and 22:6n-3 in liver, 20:5n-3, 22:5n-3, 22:6n-3 and total LC-PUFA in muscle, 22:5n-3 and 22:6n-3 in brain, and 20:4n-6, 20:5n-3, 22:6n-3 and total LC-

PUFA in eyes, were observed in fish treated with the miR-145 antagomir (Fig. 8). Among the miR-145 antagomir treatment fish, highest contents of LC-PUFA were measured in brain, followed by liver and eyes, and lowest in muscle. The results suggested that increasing *hnf4a* expression by knockdown of miR-145 promoted LC-PUFA biosynthesis in tissues of rabbitfish through up-regulation of key enzyme genes, resulting in increased LC-PUFA accumulation in brain, liver and eyes and, to a lesser extent, muscle.

#### 4. Discussion

Recently, miRNAs have been considered as critical post-transcriptional regulators of lipid metabolism genes.<sup>46</sup> Various miRNAs including miR-27a/b and miR-33a/b have been linked with regulation of lipid metabolic processes including oxidation of fatty acids, cholesterol transport, and differentiation of adipocytes in mammals.<sup>47-49</sup> However, the roles of miRNAs in the biosynthesis of LC-PUFA in vertebrates was relatively unknown but, recently, some miRNAs have been shown to target genes related to biosynthesis of LC-PUFA in rabbitfish, including miR-17 and miR-146a that directly target the  $\Delta 4$  *fads2* and *elovl5* genes, respectively, that encode key enzymes.<sup>29,32</sup> Furthermore, miR-33 and miR-24 can promote biosynthesis of LC-PUFA by targeting insulin-induced gene 1 (*insig1*) and thus facilitating the Srebp1 pathway,<sup>31,33</sup> and miR-26a mediates LC-PUFA biosynthesis through liver X receptor  $\alpha$  (Lxra)-Srebp1 pathway by targeting *lxra*.<sup>34</sup> These findings highlight the key roles of miRNAs in the post-transcriptional regulation of the metabolism of essential fatty acids in vertebrates. In

the present study, we found that miR-145, like other identified miRNAs, including miR-33 and miR-24,<sup>31,33</sup> also responds to both salinity and availability of C<sub>18</sub> PUFA precursors (e.g. ALA), and, thus, may have a potentially important role in the biosynthesis of LC-PUFA in rabbitfish. Besides its role in inhibiting proliferation of cancer cells,<sup>50,51</sup> miR-145 was shown to be involved in cholesterol metabolism and adipogenesis in mammals.<sup>40-42</sup> According to the *in vivo* expression profiles of genes related to LC-PUFA biosynthesis,<sup>17,28</sup> we found that miR-145 expression in liver displayed an inverse pattern with *hnf4α* in *S. canaliculatus* reared at different salinities or fed two different lipid diets. Furthermore, as tissue distribution of miRNAs may partly reflect miRNA functions,<sup>52</sup> we examined the tissue distribution of miR-145 and found that miR-145 was ubiquitously expressed including in liver, while the expression level of *hnf4α* was relatively highest in intestine, followed by liver.<sup>28</sup> Further *in silico* analyses found that, among the LC-PUFA biosynthesis related genes, miR-145 potentially targeted the 3'UTR of *hnf4α*, which is different from other identified miRNAs' target genes,<sup>29-34</sup> and *in vitro* luciferase reporter assays identified *hnf4α* as a novel target of miR-145 in rabbitfish. Moreover, when knocked down the miR-145, the expression of Hnf4α and LC-PUFA biosynthesis key enzymes were significantly upregulated and subsequently the accumulation of LC-PUFA were increased both in hepatocytes *in vitro* and in rabbitfish *in vivo*. Together, the results demonstrated that miR-145 is a novel mediator of biosynthesis of LC-PUFA in rabbitfish by targeting Hnf4α.

It had been established previously that Hnf4α, a ligand-dependent transcription

factor, is vital in the regulation of key enzyme genes involved in the biosynthesis of LC-PUFA in rabbitfish.<sup>26-28</sup> Previous studies have shown that activation of Hnf4 $\alpha$  by agonists (such as benfluorex and alverine) in rabbitfish primary hepatocytes or in rabbitfish *in vivo*, can increase the expression of the genes for key enzymes, including , associated with increased percentages of LC-PUFA in liver.<sup>28,53</sup> Similarly, in the present study, up-regulation of *hnf4 $\alpha$*  after knockdown of miR-145 in rabbitfish SCHL cells increased expression of *elovl5*,  $\Delta 6\Delta 5$  *fads2* and  $\Delta 4$  *fads2* and total contents of LC-PUFA. To further examine whether miR-145 regulated the key enzyme genes through targeting *hnf4 $\alpha$* , we used knockdown to reduce the expression of *hnf4 $\alpha$*  induced in SCHL cells by transfecting with miR-145 antagomir. When miR-145 was knocked down, the protein levels of Hnf4 $\alpha$  and  $\Delta 4$  Fads2 were markedly increased and this was subsequently attenuated by knockdown of *hnf4 $\alpha$* , suggesting that miR-145 might inhibit the expression of genes of LC-PUFA biosynthesis by targeting the Hnf4 $\alpha$  pathway.

It is well accepted that LC-PUFA are primarily synthesized in liver,<sup>54</sup> with LC-PUFA accumulation occurring in muscle, liver, brain and eyes.<sup>55,56</sup> Therefore, we performed fatty acid profile analysis on these tissues *in vivo* and hepatocytes *in vitro*. As expected, miR-145 knockdown up-regulated protein levels of Hnf4 $\alpha$  and  $\Delta 4$  Fads2, and subsequently increased mRNA levels of genes that are critical in the biosynthesis of LC-PUFA in cells and rabbitfish receiving the miR-145 antagomir. The mRNA levels of *hnf4 $\alpha$* , *elovl5*,  $\Delta 6\Delta 5$  *fads2* and  $\Delta 4$  *fads2* were increased in brain and eyes of fish when injected with the miR-145 antagomir. This may explain why higher contents of LC-PUFA, like ARA, EPA and DHA, were accumulated in cells and fish knocked down

miR-145 when compared to the controls. Previous studies have demonstrated that DHA is highly enriched in disk and synaptic membranes of retinal photoreceptor cells,<sup>57</sup> and when DHA was depleted from retina and brain, the cognitive and visual abilities in rhesus monkeys were markedly reduced.<sup>58,59</sup> It was found that, consistent with our previous study,<sup>34</sup> compared to the EPA and ARA, more DHA was preferentially incorporated into rabbitfish tissues, especially liver, eyes and brain, where LC-PUFA biosynthesis activity is particularly high in fish.<sup>15</sup> In the present study, as expected, DHA was particularly accumulated in brain, follow by liver and eyes. Previous studies suggested that the preferential accumulation of DHA but not ARA or EPA in these tissues may be due to the relatively lower rate of  $\beta$ -oxidation of DHA and the higher specificity for DHA of fatty acyl transferases in the tissues.<sup>55</sup>

LC-PUFA, including EPA and DHA, are antagonistic ligands of Hnf4 $\alpha$  that can modulate directly the activity of Hnf4 $\alpha$  by binding to the ligand-binding domain of Hnf4 $\alpha$  as fatty acyl-CoA thioesters.<sup>60</sup> A similar result was found in our previous study in rabbitfish<sup>17</sup>, where fish fed a FO diet (rich in LC-PUFA) showed significantly lower expression of *hnf4 $\alpha$*  and its target genes ( $\Delta 6\Delta 5fads2$ ,  $\Delta 4fads2$  and *elovl5*) than fish fed a VO diet (lacking LC-PUFA) when fish were reared at 10 ppt salinity. It seems that there is a negative feedback regulation of Hnf4 $\alpha$  in the biosynthesis of LC-PUFA. However, the liver expression of *hnf4 $\alpha$*  of rabbitfish fed the FO diet showed no difference between different salinity groups. In mammals, it is reported that the expression and activity of Hnf4 $\alpha$  are regulated by diverse extracellular and intracellular signaling pathways, and there is also extensive crosstalk with other transcription factors,

such as Ppar $\alpha$ , Ppar $\gamma$  and Srebp, to control hepatic gene expression.<sup>61,62</sup> Our previous studies and those of others have shown that expression levels of genes related to the biosynthesis of LC-PUFA, including the key enzyme genes and certain transcriptional factors, such as Srebp1 and Ppar $\gamma$ , were strongly regulated by dietary fatty acids and environmental salinity.<sup>16,17,19,62,63,64</sup> Several miRNAs, such as miR-17,<sup>29</sup> miR-24,<sup>31</sup> miR-26a,<sup>34</sup> miR-33,<sup>30</sup> miR-146a,<sup>32</sup> which have been demonstrated recently to be involved in the biosynthesis of LC-PUFA by directly targeting the relevant genes, were also responsive to dietary fatty acids and ambient salinity. It is likely that miRNA-mediated post-transcriptional modifications are among the main mechanisms whereby the expression of genes related to the biosynthesis of LC-PUFA biosynthesis are regulated by these influencing factors. Thus, there may be a combined effect of salinity and dietary fatty acids on expression of the genes encoding enzymes involved in the biosynthesis of LC-PUFA with multiple regulatory mechanisms. Similar combined effects may have impacted the expression of *hnf4a* in rabbitfish, which may explain why *hnf4a* did not always show a pattern of expression opposite to that of miR-145 in the current study and further investigation is required to clarify the mechanisms whereby salinity and nutrition regulate *hnf4a* and miR-145 in fish.

In conclusion, the current study in the marine teleost rabbitfish *S. canaliculatus* revealed a key role for miR-145 in the regulation of the biosynthesis of LC-PUFA both *in vivo* and *in vitro* through targeting *hnf4a*. The results will contribute to our knowledge of the complex regulatory mechanisms of the biosynthesis and metabolism of LC-PUFA. In the long-term, these findings might be helpful in developing practical

solutions to enhance the quality of aquacultured fish by increasing the production and accumulation of LC-PUFA.

### **Author contributions**

Cuiying Chen and Mei Zhang conceived and designed the experiments; Cuiying Chen, Yu Hu, Mei Zhang and Xianda He performed the experiments; Cuiying Chen, Yuanyou Li, Shuqi Wang, Dizhi Xie, and Cuihong You analyzed and/or interpreted data; Cuiying Chen, Mei Zhang, Xiaobo Wen, Jiajian Shen, Óscar Monroig, and Douglas R. Tocher wrote and revised the paper.

### **Funding**

This work was financially supported by the National Natural Science Foundation of China (No.31702357), National Key R&D Program of China (2018YFD0900400), Natural Science Foundation of Guangdong Province (2020A1515011252) and the STU Scientific Research Foundation for Talents (No. NTF19019).

### **Conflict of interest**

The authors declare no conflict of interests and no permission is required for publication.

### **Acknowledgments**

We are very grateful to our team members for the technical advice and valuable assistance during the feeding trial and sample analysis.



## References

- (1) Calder, P. C. N-3 fatty acids, inflammation and immunity: new mechanisms to explain old actions. *Proc. Nutr. Soc.* 2013, 72, 326–336.
- (2) Campoy, C.; Escolano-Margarit, M. V.; Anjos, T.; Szajewska, H.; Uauy, R. Omega 3 fatty acids on child growth, visual acuity and neurodevelopment. *Br. J. Nutr.* 2012, 107, S85–S106.
- (3) Delgado-Lista, J.; Perez-Martinez, P.; Lopez-Miranda, J.; Perez Jimenez, F. Long chain omega-3 fatty acids and cardiovascular disease: a systematic review. *Br. J. Nutr.* 2012, 107, S201–S213.
- (4) Gil, A.; Serra-Majem, L.; Calder, P. C.; Uauy, R. Systematic reviews of the role of omega-3 fatty acids in the prevention and treatment of disease. *Br. J. Nutr.* 2012, 107, S1–S2.
- (5) Castro, L. F.; Tocher, D. R.; Monroig, Ó. Long-chain polyunsaturated fatty acid biosynthesis in chordates: Insights into the evolution of Fads and Elovl gene repertoire. *Prog. Lipid Res.* 2016, 62, 25-40.
- (6) Tocher, D. R. Omega-3 long-chain polyunsaturated fatty acids and aquaculture in perspective. *Aquaculture* 2015, 449, 94-107.
- (7) Monroig, Ó.; Tocher, D. R.; Castro, L. F. C. Polyunsaturated fatty acid biosynthesis and metabolism in fish. In: Burdge, G.C. (Ed.), *Polyunsaturated Fatty Acid Metabolism*, Academic Press and AOCS Press, London, 2018, pp. 31–60.
- (8) Lopes-Marques, M.; Kabeya, N.; Qian, Y.; Ruivp, R.; Santos, M.; Venkatesh, B. Retention of fatty acyl desaturase 1 (*fads1*) in *Elopomorpha* and *Cyclostomata* provides novel insights into the evolution of long-chain polyunsaturated fatty acid biosynthesis in vertebrates. *BMC Evol. Biol.* 2018, 18, 157.
- (9) Li, Y.; Wen, Z. Y.; You, C. H.; Xie, D. Z.; Tocher, D. R.; Zhang, Y. L.; Wang, S. Q.; Li, Y. Y. Genome wide identification and functional characterization of two LC-PUFA biosynthesis elongase (*elovl8*) genes in rabbitfish (*Siganus canaliculatus*). *Aquaculture* 2020, 522: 735127.
- (10)FAO. The State of World Fisheries and Aquaculture (SOFIA): Contributing to food

535 security and nutrition for all, Rome: Food and Agriculture Organization 2016.

536 (11) Turchini, G. M.; Torstensen, B. E.; Ng, W. K. Fish oil replacement in finfish  
537 nutrition. *Rev. Aquacult.* 2009, 1, 10–57.

538 (12) Olsen, Y. Resources for fish feed in future mariculture. *Aquacult. Env. Interac.*  
539 2011, 1, 187–200.

540 (13) Nasopoulou, C.; Zaetakis, I. Benefits of fish oil replacement by plant originated  
541 oils in compounded fish feeds. *LWT-Food Technol.* 2012, 47, 217–224.

542 (14) Li, Y. Y.; Hu, C. B.; Zheng, Y. J.; Xia, X. A.; Xu, W. J.; Wang, S. Q. The effects  
543 of dietary fatty acids on liver fatty acid composition and  $\Delta 6$ -desaturase expression differ  
544 with ambient salinities in *Siganus canaliculatus*. *Comp. Biochem. Physiol. B. Biochem.*  
545 *Mol. Biol.* 2008, 151, 183–190.

546 (15) Monroig, Ó.; Wang, S. Q.; Zhang, L.; You, C. H.; Tocher, D. R.; Li, Y. Y.  
547 Elongation of long-chain fatty acids in rabbitfish *Siganus canaliculatus*: Cloning,  
548 functional characterisation and tissue distribution of Elovl5- and Elovl4-like elongases.  
549 *Aquaculture* 2012, 350–353.

550 (16) Zheng, X.; Torstensen, B. E.; Tocher, D. R.; Dick, I. R.; Bell, J. G. Environmental  
551 and dietary influences on highly unsaturated fatty acid biosynthesis and expression of  
552 fatty acyl desaturase and elongase genes in liver of Atlantic salmon (*Salmo salar*).  
553 *Biochim. Biophys. Acta-Mol. Cell Biol. L.* 2005, 1734, 13–24.

554 (17) Xie, D. Z.; Wang, S. Q.; You, C. H.; Chen, F.; Tocher, D. R.; Li, Y. Y.  
555 Characteristics of LC-PUFA biosynthesis in marine herbivorous teleost *Siganus*  
556 *canaliculatus* under different ambient salinities. *Aquac. Nutr.* 2015, 2, 541–551.

557 (18) Leaver, M. J.; Villeneuve, L. A.; Obach, A. Functional genomics reveals increases  
558 in cholesterol biosynthetic genes and highly unsaturated fatty acid biosynthesis after  
559 dietary substitution of fish oil with vegetable oils in Atlantic salmon (*Salmo salar*).  
560 *BMC Genomics* 2008, 9, 299.

561 (19) Zhang, Q. H.; You, C. H.; Liu, F.; Zhu, W. D.; Wang, S. Q.; Xie, D. Z.; Monroig,  
562 Ó.; Tocher, D. R.; Li, Y. Y. Cloning and characterization of Lxr and Srebp1, and their  
563 potential roles in regulation of LC-PUFA biosynthesis in rabbitfish *Siganus*  
564 *canaliculatus*. *Lipids* 2016, 51, 1–13.

565 (20) Li, Y. Y.; Zhao, J. H.; Dong, Y. W.; Yin, Z. Y.; Li, Y.; Liu, Y.; You, C. H.;  
 566 Monroig, Ó.; Tocher, D. R.; Wang, S. Q. Sp1 is involved in vertebrate LC-PUFA  
 567 biosynthesis by up-regulating the expression of liver desaturase and elongase genes. *Int.*  
 568 *J Mol. Sci.* 2019, 20, 5066.

569 (21) Li, Y. Y.; Yin, Z. Y.; Dong, Y. W.; Wang, S. Q.; Monroig, Ó.; Tocher, D. R. Ppar $\gamma$  is  
 570 involved in the transcriptional regulation of liver LC-PUFA biosynthesis by targeting  
 571 the  $\Delta 6\Delta 5$  fatty acyl desaturase gene in the marine teleost *Siganus canaliculatus*. *Mar.*  
 572 *Biotechnol.* 2019, 21, 19–29.

573 (22) Hwang-Verslues, W. W.; Sladek, F. M. HNF4 $\alpha$ --role in drug metabolism and  
 574 potential drug target? *Curr. Opin. Pharmacol.* 2010, 10, 698-705.

575 (23) Martinez-Jimenez, C. P.; Kymizi, I.; Cardot, P.; Gonzalez, F. J.; Talianidis, I.  
 576 Hepatocyte nuclear factor 4 $\alpha$  coordinates a transcription factor network regulating  
 577 hepatic fatty acid metabolism. *Mol. Cell. Biol.* 2010, 30, 565–577.

578 (24) Yin, L. Y.; Ma, H. Y.; Ge, X. M.; Edwards, P. A.; Zhang, Y. Q. Hepatic hepatocyte  
 579 nuclear factor 4 $\alpha$  is essential for maintaining triglyceride and cholesterol homeostasis.  
 580 *Arterioscler. Thromb. Vasc. Biol.* 2011, 31, 328–336.

581 (25) Hayhurst, G. P.; Lee, Y. H.; Lambert, G.; Ward, J. M.; Gonzalez, F. J. Hepatocyte  
 582 nuclear factor 4 (nuclear receptor 2A1) is essential for maintenance of hepatic gene  
 583 expression and lipid homeostasis. *Mol. Cell. Biol.* 2001, 21, 1393–1403.

584 (26) Dong, Y. W.; Wang, S. Q.; Chen, J. L.; Zhang, Q. H.; Liu, Y.; You, C. H.;  
 585 Monroig, Ó.; Tocher, D. R.; Li, Y. Y. Hepatocyte nuclear factor 4 $\alpha$  (HNF4 $\alpha$ ) is a  
 586 transcription factor of vertebrate fatty acyl desaturase gene as identified in marine  
 587 teleost *Siganus canaliculatus*. *PLoS One* 2016, 11, e0160361.

588 (27) Dong, Y. W.; Zhao, J. H.; Chen, J. L.; Wang, S. Q.; Liu, Y.; Zhang, Q. H.; You, C.  
 589 H.; Monroig, Ó.; Tocher, D. R.; Li, Y. Y. Cloning and characterization of  $\Delta 6/\Delta 5$  fatty  
 590 acyl desaturase (Fad) gene promoter in the marine teleost *Siganus canaliculatus*. *Gene*  
 591 2018, 647, 174–180.

592 (28) Wang, S. Q.; Chen, J. L.; Jiang, D. L.; Zhang, Q. H.; You, C. H.; Monroig, Ó.;  
 593 Tocher, D. R.; Li, Y. Y. Hnf4 $\alpha$  is involved in the regulation of vertebrate LC-PUFA  
 594 biosynthesis: Insights into the regulatory role of Hnf4 $\alpha$  on expression of liver fatty acyl

desaturases in the marine teleost *Siganus canaliculatus*. *Fish Physiol. Biochem.* 2018, 44, 805–815.

(29) Zhang, Q. H.; Xie, D. Z.; Wang, S. Q.; You, C. H.; Monroig, Ó.; Tocher, D. R.; Li, Y. Y. MiR-17 is involved in the regulation of LC-PUFA biosynthesis in vertebrates: Effects on liver expression of a fatty acyl desaturase in the marine teleost *Siganus canaliculatus*. *Biochim. Biophys. Acta-Mol. Cell Biol. L.* 2014, 1841, 934–943.

(30) Zhang, Q. H.; You, C. H.; Wang, S. Q.; Dong, Y. W.; Monroig, Ó.; Tocher, D. R.; Li, Y. Y. The miR-33 gene is identified in a marine teleost: A potential role in regulation of LC-PUFA biosynthesis in *Siganus canaliculatus*. *Sci. Rep.* 2016, 6, 32909.

(31) Chen, C. Y.; Wang, S. Q.; Zhang, M.; Chen, B. J.; You, C. H.; Xie, D. Z.; Liu, Y.; Monroig, Ó.; Tocher, D. R.; Waiho, K.; Li, Y. Y. MiR-24 is involved in vertebrate LC-PUFA biosynthesis as demonstrated in marine teleost *Siganus canaliculatus*. *Biochim. Biophys. Acta-Mol. Cell Biol. L.* 2019, 1864, 619–628.

(32) Chen, C. Y.; Zhang, J. Y.; Zhang, M.; You, C. H.; Liu, Y.; Wang, S. Q.; Li, Y. Y. MiR-146a is involved in the regulation of vertebrate LC-PUFA biosynthesis by targeting *elovl5* as demonstrated in rabbitfish *Siganus canaliculatus*. *Gene* 2018, 676, 306–314.

(33) Sun, J. J.; Zheng, L. G.; Chen, C. Y.; Zhang, J. Y.; You, C. H.; Zhang, Q. H.; Ma, H. Y.; Monroig, Ó.; Tocher, D. R.; Wang, S. Q.; Li, Y. Y. MicroRNAs involved in the regulation of LC-PUFA biosynthesis in teleosts: MiR-33 enhances LC-PUFA biosynthesis in *Siganus canaliculatus* by targeting *insig1* which in turn upregulates *srebpl*. *Mar. Biotechnol.* 2019, 21, 475–487.

(34) Chen, C. Y.; Wang, S. Q.; Hu, Y.; Zhang, M.; He, X. D.; You, C. H.; Wen, X. B.; Monroig, Ó.; Tocher, D. R.; Li, Y. Y. MiR-26a mediates LC-PUFA biosynthesis by targeting the *Lxra-Srebpl* pathway in the marine teleost *Siganus canaliculatus*. *JBC* 2020, 295, 13875–13886.

(35) Rayner, K. J.; Fernandez-Hernando, C.; Moore, K. J. MicroRNAs regulating lipid metabolism in atherogenesis. *Thromb Haemost* 2012, 107, 642–647.

(36) Chi, W.; Tong, C. B.; Gan, X. N.; He, S. P. Characterization and comparative profiling of MiRNA transcriptomes in bighead carp and silver carp. *PLoS One* 2011, 6,

625 e23549.

626 (37) Fernandez-Hernando, C.; Suarez, Y.; Rayner, K. J.; Moore, K. J. MicroRNAs in  
627 lipid metabolism. *Curr. Opin. Lipidol.* 2011, 22, 86–92.

628 (38) Sacco, J.; Adeli, K. MicroRNAs: Emerging roles in lipid and lipoprotein  
629 metabolism. *Curr. Opin. Lipidol.* 2012, 23, 220–225.

630 (39) Soh, J.; Iqbal, J.; Queiroz, J.; Fernandez-Hernando, C.; Hussain, M. MicroRNA-  
631 30c reduces hyperlipidemia and atherosclerosis in mice by decreasing lipid synthesis  
632 and lipoprotein secretion. *Nat. Med.* 2013, 19, 892–900.

633 (40) Kang, M. H.; Zhang, L. H.; Wijesekara, N.; Haan, W.; Butland, S.; Bhattacharjee,  
634 A.; Hayden, M. R. Regulation of ABCA1 protein expression and function in hepatic  
635 and pancreatic islet cells by miR-145. *Arterioscler. Thromb. Vasc. Biol.* 2013, 33,  
636 2724–2732.

637 (41) Guo, Y.; Chen, Y.; Zhang, Y.; Chen, L.; Mo, D. Up-regulated miR-145 expression  
638 inhibits porcine preadipocytes differentiation by targeting IRS1. *Int. J. Biol. Sci.* 2012,  
639 8, 1408–1417.

640 (42) Lin, Y. Y.; Chou, C. F.; Giovarelli, M.; Briata, P.; Gherzi, R.; Chen, C. Y. KSRP  
641 and MicroRNA-145 are negative regulators of lipolysis in white adipose tissue. *Mol.*  
642 *Cell. Biol.* 2014, 34, 2339–49.

643 (43) Liu, Y.; Zhang, Q. H.; Dong, Y. W. You, C. H.; Wang, S. Q.; Li, Y. Q.; Li, Y. Y.  
644 Establishment of a hepatocyte line for studying biosynthesis of long chain  
645 polyunsaturated fatty acids from a marine teleost, the white spotted spinefoot *Siganus*  
646 *canaliculatus*. *J. Fish Biol.* 2017, 91, 603–616.

647 (44) Krutzfeldt, J. Silencing of microRNAs *in vivo* with ‘antagomirs’. *Nature* 2005,  
648 438, 685–689.

649 (45) Ou, J.; Tu, H.; Shan, B.; Luk, A.; DeBose-Boyd, R. A.; Bashmakov, Y.; Goldstein,  
650 J. L.; Brown, M. S. Unsaturated fatty acids inhibit transcription of the sterol regulatory  
651 element-binding protein-1c (SREBP-1c) gene by antagonizing ligand-dependent  
652 activation of the LXR. *Proc. Natl. Acad. Sci. U. S. A.* 2001, 98, 6027–6032.

653 (46) Flowers, E.; Froelicher, E. S.; Aouizerat, B. E. MicroRNA regulation of lipid  
654 metabolism. *Metabolism* 2013, 62, 12–20.

655 (47) Karbiener, M.; Fischer, C.; Nowitsch, S.; Opriessing, P.; Papak, C.; Ailhaud, G.;  
 656 Dain, C.; Amri, E.; Scheideler, M. MicroRNA miR-27b impairs human adipocyte  
 657 differentiation and targets PPAR $\gamma$ . *Biochem. Biophys. Res. Commun.* 2009, 390, 247–  
 658 251.

659 (48) Kim, S. Y.; Kim, A. Y.; Lee, H. W. Son, Y. H.; Lee, G. Y.; Lee, J.; Lee, Y. S.; Kim,  
 660 J. B. MiR-27a is a negative regulator of adipocyte differentiation via suppressing  
 661 PPAR $\gamma$  expression. *Biochem. Biophys. Res. Commun.* 2010, 392, 323–328.

662 (49) Davalos, A.; Goedeke, L.; Smibert, P.; Ramirez, C. M.; Warriar, N. P.; Andreo, U.;  
 663 Rayner, K.; Suresh, U.; Moore, K. J.; Suarez, Y.; Lai, E. C.; Fernandez-Hernando, C.  
 664 MiR-33a/b contribute to the regulation of fatty acid metabolism and insulin signaling.  
 665 *Proc. Natl. Acad. Sci. U. S. A.* 2011, 108, 9232–9237.

666 (50) Sachdeva, M.; Mo, Y. Y. MicroRNA-145 suppresses cell invasion and metastasis  
 667 by directly targeting mucin 1. *Cancer Res.* 2010, 70:378-87.

668 (51) Shi, B.; Sepp-Lorenzino, L.; Prisco, M.; Linsley, P.; Angelis, T.; Baserga, R.  
 669 MicroRNA-145 targets the insulin receptor substrate-1 and inhibits the growth of colon  
 670 cancer cells. *J. Biol. Chem.* 2007, 282, 32582-90.

671 (52) Lagosquintana, M.; Rauhut, R.; Yalcin, A.; Meyer, J.; Lendeckel, W.; Tuschl, T.  
 672 Identification of tissue-specific microRNAs from mouse. *Curr. Biol.* 2002, 12, 735–739.

673 (53) Li, Y. Y.; Zeng, X. W.; Dong, Y. W.; Chen, C. Y.; Tang, G. X.; Chen, J. L. Hnf4 $\alpha$   
 674 is involved in LC-PUFA biosynthesis by up-regulating gene transcription of elongase  
 675 in marine teleost *Siganus canaliculatus*. *Int. J. Mol. Sci.* 2018, 19, 3193.

676 (54) Xu, H. G.; Dong, X. J.; Ai, Q. H.; Mai, K. S.; Xu, W.; Zhang, Y. J.; Zuo, R. T.  
 677 Regulation of tissue LC-PUFA contents,  $\Delta 6$  fatty acyl desaturase (*fads2*) gene  
 678 expression and the methylation of the putative *fads2* gene promoter by different dietary  
 679 fatty acid profiles in Japanese seabass (*lateolabrax japonicus*). *PLoS One* 2014, 9,  
 680 e87726.

681 (55) Bell, J. G.; Tocher, D. R.; Henderson, R. J. Altered fatty acid compositions in  
 682 Atlantic salmon (*Salmo salar*) fed diets containing linseed and rapeseed oils can be  
 683 partially restored by a subsequent fish oil finishing diet. *J. Nutr.* 2003, 133, 2793–2801.

684 (56) Zhang, M.; Chen, C. Y.; You, C. H.; Chen, B. J.; Wang, S. Q.; Li, Y. Y. Effects of  
685 dietary docosahexaenoic to eicosapentaenoic acid ratio (DHA/EPA) on growth,  
686 immune indices, tissue fatty acid composition and expression of LC-PUFA biosynthesis  
687 related genes in juvenile golden pompano *Trachinotus ovatus*. *Aquaculture* 2019, 488-  
688 495.

689 (57) Bell, M. V.; Tocher, D. R. Molecular species composition of the major  
690 phospholipids in brain and retina from rainbow trout (*Salmo gairdneri*). *Biochem. J.*  
691 1989, 264, 909–915.

692 (58) Connor, W.; Neuringer, M.; Barstad, L. Dietary deprivation of linolenic acid in  
693 rhesus monkeys: Effects on plasma and tissue fatty acid composition and on visual  
694 function. *Trans. Assoc. Am. Phys.* 1984, 97, 1–9.

695 (59) Neuringer, M.; Connor, W. E.; Petten, C.; Barstad, L. Dietary omega-3 fatty acid  
696 deficiency and visual loss in infant rhesus monkeys. *J. Clin. Investig.* 1984, 73, 272–  
697 276.

698 (60) Hertz, R.; Magenheimer, J.; Berman, I.; Bar-Tana, J. Fatty acyl-CoA thioesters are  
699 ligands of hepatic nuclear factor 4 $\alpha$ . *Nature* 1997, 392, 512–516.

700 (61) Lu, H. Crosstalk of Hnf4 $\alpha$  with extracellular and intracellular signaling pathways  
701 in the regulation of hepatic metabolism of drugs and lipids. *Acta Pharm. Sin. B.* 2016,  
702 6, 393-408.

703 (62) Martinez-Jimenez, C. P.; Kyrmizi, I.; Cardot, P.; Gonzalez, F. J.; Talianidis, I.  
704 Hepatocyte nuclear factor 4 coordinates a transcription factor network regulating  
705 hepatic fatty acid metabolism. *Mol. Cell Biol.* 2009, 30, 565-577.

706 (63) Vagner, M.; Santigosa, E. Characterization and modulation of gene expression and  
707 enzymatic activity of delta-6 desaturase in teleosts: A review. *Aquaculture* 2011, 315,  
708 131–143.

709 (64) You, C. H.; Jiang, D. L.; Zhang, Q. H.; Xie, D. Z.; Wang, S. Q.; Dong, Y. W.; Li,  
710 Y. Y. Cloning and expression characterization of peroxisome proliferator-activated  
711 receptors (PPARs) with their agonists, dietary lipids, and ambient salinity in rabbitfish  
712 *Siganus canaliculatus*. *Comp. Biochem. Physiol. B. Biochem. Mol. Biol.* 2017, 206: 54–  
713 64.

## TABLES

**Table 1**

The fatty acid composition (% total fatty acid) of rabbitfish *S. canaliculatus* hepatocyte line (SCHL) <sup>\*</sup>.

Fatty acid	Mock cells <sup>#</sup>	NC antagomir	miR-145 antagomir	P-value
16:0	15.71 ± 3.00	14.04 ± 0.30	12.41 ± 0.31	0.010
18:0	14.65 ± 0.07	14.87 ± 0.39	13.38 ± 0.17	0.013
16:1n-7	1.28 ± 0.09	1.54 ± 0.12	1.37 ± 0.02	0.208
16:1n-9	1.50 ± 0.16	1.72 ± 0.06	1.65 ± 0.07	0.482
18:1n-9	22.06 ± 1.01	20.72 ± 0.73	21.36 ± 0.17	0.420
20:1n-9	0.46 ± 0.01	0.53 ± 0.05	0.46 ± 0.03	0.290
18:2n-6 (LA)	2.85 ± 0.34	3.86 ± 0.47	3.60 ± 0.12	0.620
18:3n-6	0.21 ± 0.00	0.21 ± 0.00	0.31 ± 0.03	0.375
20:2n-6	1.13 ± 0.47	1.28 ± 0.15	1.59 ± 0.15	0.192
20:3n-6	1.33 ± 0.02	1.43 ± 0.06	1.49 ± 0.02	0.392
20:4n-6 (ARA)	7.49 ± 1.39	7.10 ± 0.11	7.57 ± 0.07	0.011
22:4n-6	0.58 ± 0.00	0.69 ± 0.07	0.72 ± 0.01	0.688
18:3n-3 (ALA)	2.10 ± 0.53	2.13 ± 0.23	1.88 ± 0.08	0.342
20:3n-3	1.03 ± 0.51	1.10 ± 0.29	0.64 ± 0.02	0.157
20:4n-3	0.28 ± 0.06	0.34 ± 0.02	0.33 ± 0.01	0.445
20:5n-3 (EPA)	2.33 ± 0.14	2.37 ± 0.11	2.82 ± 0.02	0.008
22:5n-3	1.94 ± 0.23	2.28 ± 0.17	2.68 ± 0.09	0.076
22:6n-3(DHA)	7.39 ± 0.05	7.24 ± 0.09	9.08 ± 0.08	0.000
SFA	30.36 ± 3.07	28.91 ± 0.68	25.79 ± 0.48	0.009
MUFA	25.29 ± 1.25	24.51 ± 0.64	24.85 ± 0.12	0.625
PUFA	28.68 ± 2.90	29.89 ± 0.78	32.56 ± 0.19	0.016
LC-PUFA	23.51 ± 2.14	23.84 ± 0.49	26.92 ± 0.16	0.001
n-6 LC-PUFA	10.53 ± 1.88	10.51 ± 0.28	11.36 ± 0.16	0.039
n-3 LC-PUFA	12.97 ± 0.25	13.34 ± 0.38	15.56 ± 0.08	0.001

<sup>\*</sup> SCHL cells were incubated with 30 μM ALA for further 48 h after transfection with 20 nM NC antagomir or miR-145 antagomir for 24h. Data presented as mean ± SEM (n = 4). SFA, saturated fatty acids; MUFA, monounsaturated fatty acids; PUFA, polyunsaturated fatty acids; LC-PUFA, long-chain polyunsaturated fatty acids including 20:2n-6, 20:3n-3, 20:4n-3, 20:5n-3, 22:5n-3, 22:6n-3, 20:3n-6, 20:4n-6 and 22:4n-6.

<sup>#</sup> Mock cells, SCHL cells were incubated with 30 μM ALA for further 48 h after transfection without any oligonucleotides for 24 h.



## FIGURES

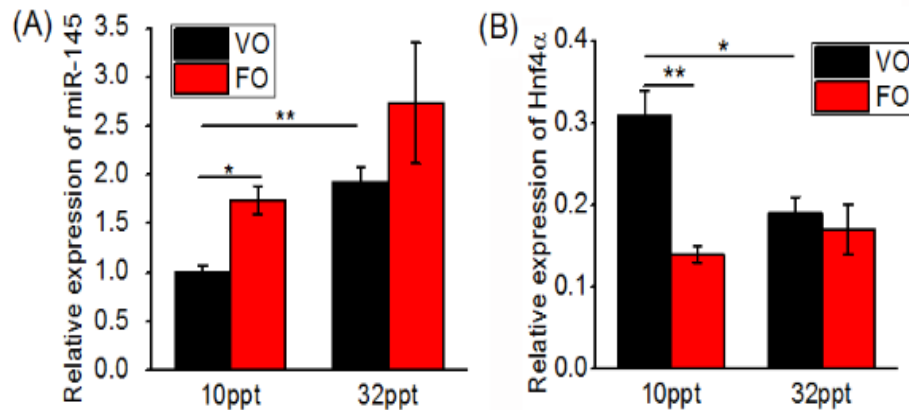


**Fig 1. Abundance of miR-145 and *hnf4α* in liver of rabbitfish fed two diets (fish oil or vegetable oil, FO or VO as lipid resource) at two salinities (10 ppt and 32 ppt).**

Expression levels of miR-145 (A) and Hnf4α (B) determined by real-time quantitative PCR (qPCR) and normalized to 18S rRNA or β-actin respectively. Data are means ± SEM as fold change relative to the fish fed diets with VO at 10 ppt salinity. \*  $P < 0.05$ ,

\*\*  $P < 0.01$ .

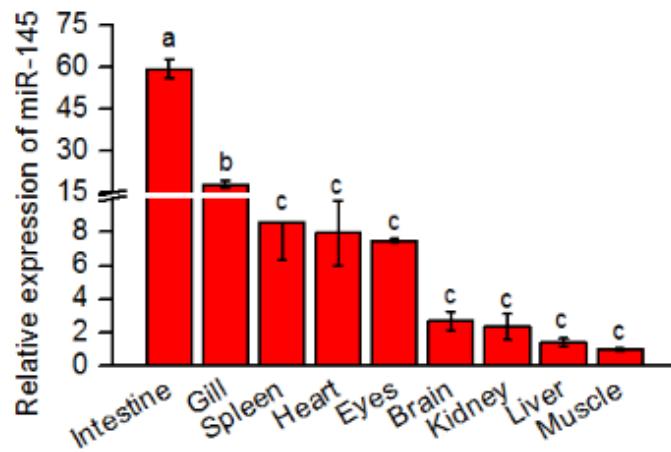


**Fig 2. Relative tissue distribution profile of miR-145 in *S. canaliculatus* determined by qPCR.** Data are means  $\pm$  SEM (n = 6) relative to the level in muscle (=1), and different letters above bars show significant differences ( $P < 0.05$ ) among the analyzed tissues.

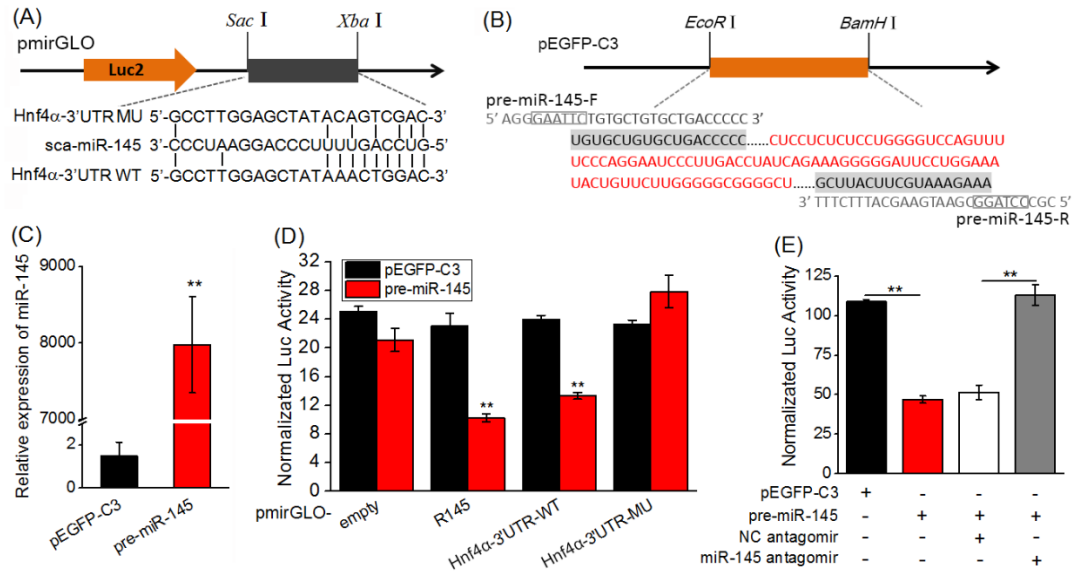


**Fig 3. Rabbitfish *hnf4α* is a target of miR-145.** Sequence alignment of *hnf4α* (A) and pre-miR-145 (B), and the construction plasmids. (C) Rabbitfish miR-145 was overexpressed in HEK 293T cells by transfecting with the pre-miR-145 expression plasmid. (D) Luciferase activity in HEK 293T cells co-transfected with pre-miR-145 or pEGFP-C3 plasmid with different recombinant dual-luciferase reporter vectors: pmirGLO-empty as negative control; pmirGLO-R145 as positive control; pmirGLO-Hnf4α-3'UTR-WT containing wild type of *hnf4α* 3'UTR; pmirGLO-Hnf4α-3'UTR-MU with site-directed mutation in 3'UTR of *hnf4α*. (E) HEK 293T cells were co-transfected with pre-miR-145 or pEGFP-C3 plasmid and miR-145 antagomir or NC antagomir. The luciferase activity was determined and normalized to the activity of renilla luciferase. Data are presented as means  $\pm$  SEM (n = 6) from a least two independent experiments. \*  $P < 0.05$ , \*\*  $P < 0.01$  versus the controls.

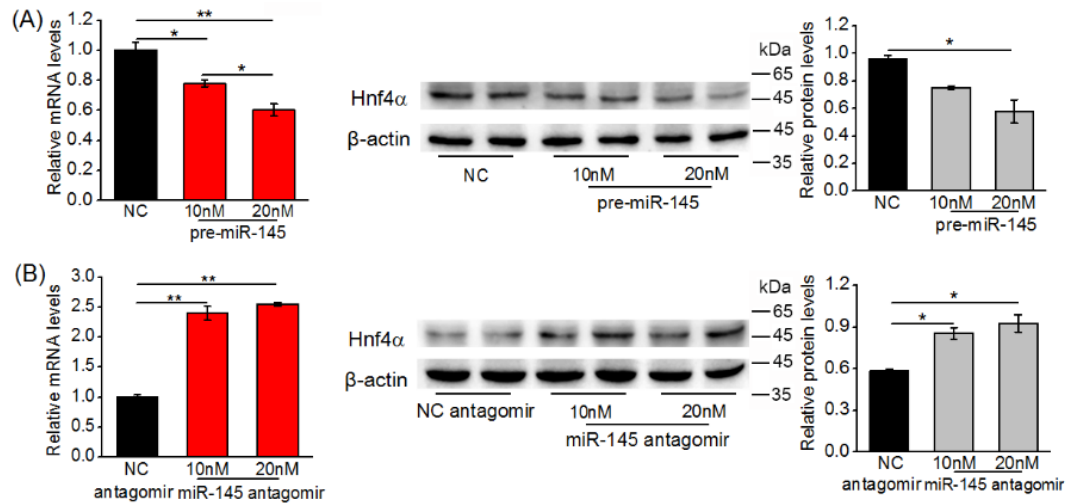


**Fig 4. MiR-145 decreased the abundance of *hnf4α* at both mRNA and protein level.**

(A) Rabbitfish SCHL cells were transfected with pre-miR-145 or its negative control oligonucleotides within the concentration gradient. After 24 h, the level of *hnf4α* mRNA (left) was examined by qPCR and normalized to  $\beta$ -actin. After 48 h, aliquots of protein from cells were loaded on 10 % SDS-PAGE and the blot was immunoprobed with monoclonal antibody specified for rabbitfish Hnf4α (~50 kDa) and normalized to  $\beta$ -actin (~42 kDa) (middle and right) as described in Materials and Methods. (B) Rabbitfish SCHL cells were transfected with miR-145 antagomir or NC-antagomir with concentration gradient. After 24 h, the level of *hnf4α* mRNA (left) was examined by qPCR as described above. After 48 h, the Hnf4α protein levels (middle and right) were determined by Western blotting as described above. The intensity of the Western blotting bands was quantified by Image Studio Software (version 5.2, LI-COR). The intensity ratio of Hnf4α/ $\beta$ -actin was calculated as an indication of endogenous Hnf4α protein expression change. Data are means  $\pm$  SEM of triplicate treatments as fold change from the controls. \*  $P < 0.05$ , \*\*  $P < 0.01$ .

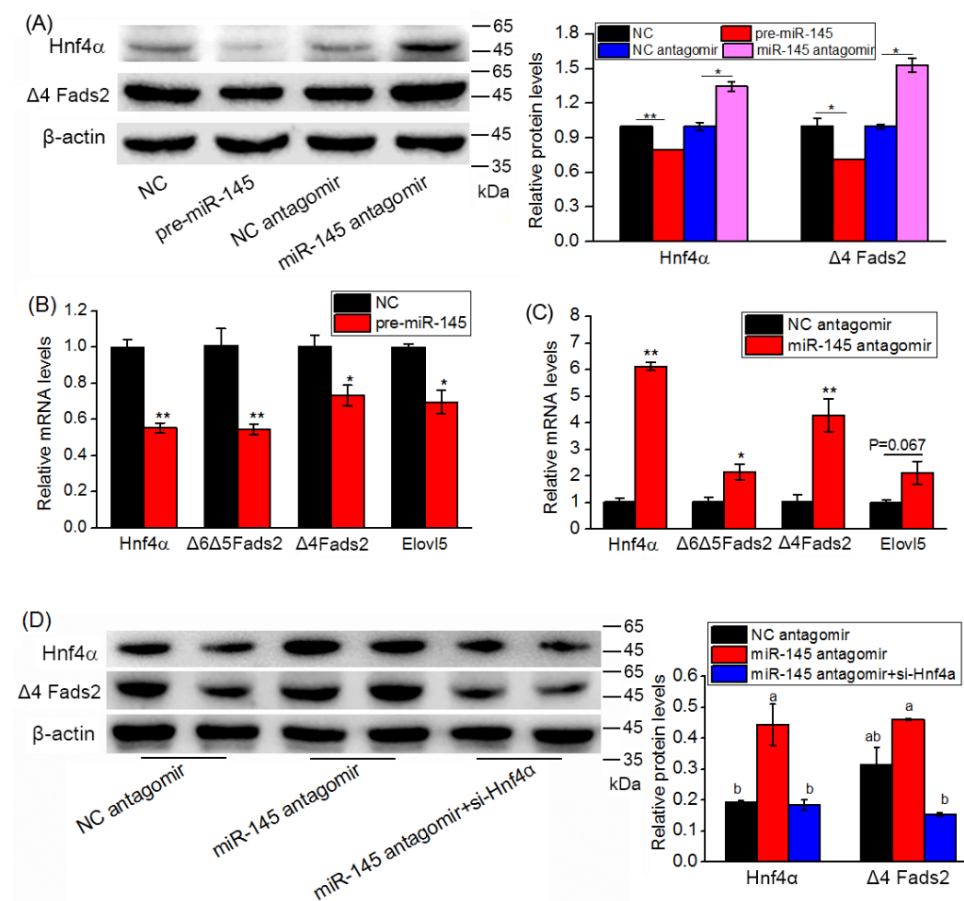


**Fig 5. The inhibitory role of miR-145 on the expression of genes involved in LC-PUFA biosynthesis is by mediating *hnf4α*.** (A) Rabbitfish SCHL cells were transfected with 20 nM pre-miR-145 or its control and 20 nM miR-145 antagomir or NC antagomir. After 48 h, aliquots of protein from cells were subjected to immunoblot analysis of the protein levels of Hnf4α and Δ4 Fads2 (~49 kDa) as above. (B, C) After SCHL cells transfected with 20 nM pre-miR-145 or its control and 20 nM miR-145 antagomir or NC antagomir for 24 h, the mRNA levels of *hnf4α*, *Δ4 fads2*, *Δ6Δ5 fads2* and *elovl5* were analyzed by qPCR. (D) Rabbitfish SCHL cells were transfected with 20 nM miR-145 antagomir or NC antagomir or co-transfected with 20 nM miR-145 antagomir and si-hnf4α. After 48 h, the protein levels of Hnf4α and Δ4 Fads2 were determined by Western blotting as above. The intensity of the Western blotting bands

796 was quantified by Image Studio Software (version 5.2, LI-COR). Data are means  $\pm$   
797 SEM of triplicate treatments as fold change from the controls. \*  $P < 0.05$ , \*\*  $P < 0.01$   
798 versus the controls and different superscripts in the same columns indicate significant  
799 differences at  $P < 0.05$ .

800

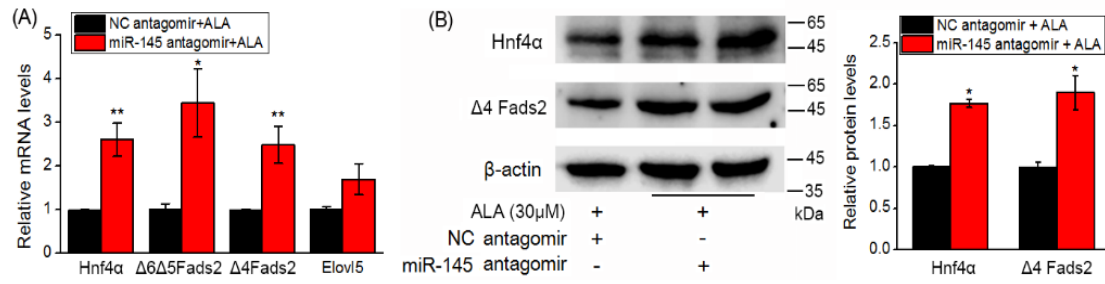


**Fig 6. Knockdown of miR-145 increased LC-PUFA biosynthesis in SCHL cells.**

SCHL cells were transfected with 20 nM miR-145 antagomir or NC antagomir for 24 hours, and then incubated with 30 μM precursor ALA for further 48 h. (A) The levels of *hnf4α*, *Δ4 fads2*, *Δ6Δ5 fads2* and *elovl5* mRNAs were determined by qPCR. (B) The protein levels of Hnf4α and Δ4 Fads2 were analyzed by Western blotting. The intensity of the bands was quantified by Image Studio Software (version 5.2, LI-COR). Data are presented as means ± SEM of at least triplicate treatments as fold change from the controls. \*  $P < 0.05$ , \*\*  $P < 0.01$  versus the controls.

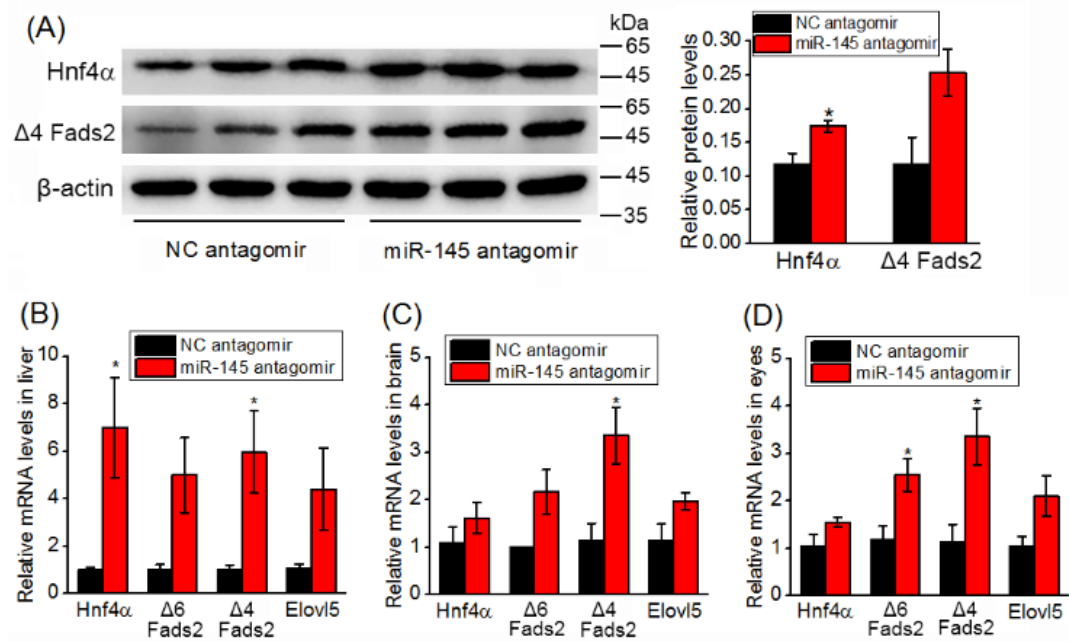


**Fig 7. Knockdown of miR-145 increased LC-PUFA biosynthesis in rabbitfish by facilitating Hnf4α activation.** The rabbitfish were treated with miR-145 antagomirs or NC antagomir twice weekly for 3 weeks. (A) The protein levels of Hnf4α and Δ4 Fads2 were determined by Western blotting. The levels of *hnf4α*, *Δ6Δ5 fads2*, *Δ4 fads2* and *elovl5* mRNAs in liver (B), brain (C) and eyes (D) were determined by qPCR. Data are presented as mean ± SEM (n = 4). \*  $P < 0.05$ , \*\*  $P < 0.01$  versus the controls.



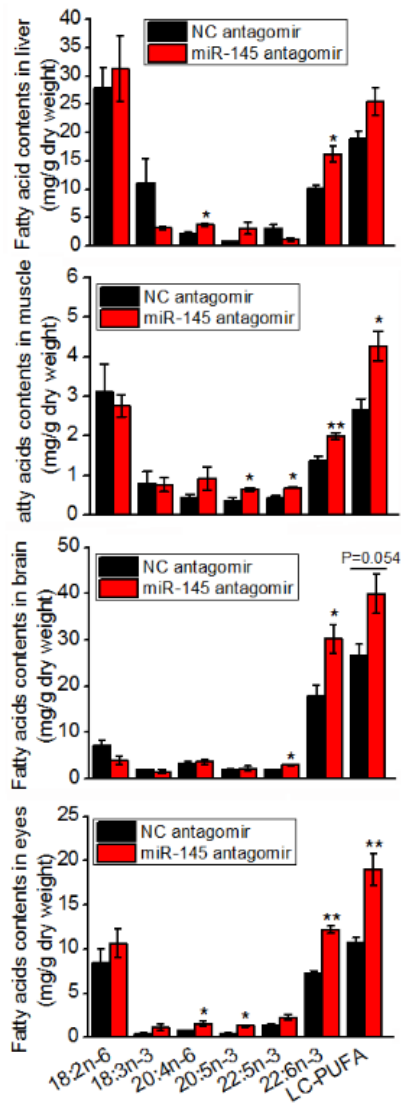


**Fig 8. Knockdown of miR-145 increased LC-PUFA accumulation in tissues of rabbitfish.** The fatty acid contents of liver, muscle, brain and eyes were analyzed by gas chromatography (GC). Individual fatty acids were identified by comparing with the known commercial standards (Sigma, USA) and the content of each fatty acid (mg) relative to dry weight of tissues (g) was calculated using a 17:0 internal standard. Data are presented as means  $\pm$  SEM (n = 4). \*  $P < 0.05$ , \*\*  $P < 0.01$  versus the controls.